Pure Appl. Chem., Vol. 79, No. 9, pp. 1505–1519, 2007.
doi:10.1351/pac200779091505

Synthesis and characterization of micrometer-sized molecularly imprinted spherical polymer particulates prepared via precipitation polymerization*

Jinfang Wang[1], Peter A. G. Cormack[1,‡], David C. Sherrington[1], and Ezat Khoshdel[2]

[1]WestCHEM, Department of Pure and Applied Chemistry, University of Strathclyde, Thomas Graham Building, 295 Cathedral Street, Glasgow, G1 1XL, UK; [2]Unilever Research, Port Sunlight, Quarry Road East, Bebington, Wirral, CH63 3JW, UK

Abstract: In this paper, the synthesis and characterization of molecularly imprinted spherical polymer particulates prepared via precipitation polymerization is described. The effects of the monomer and initiator concentrations and the solvent on the polymerizations were investigated systematically. Polymer microspheres with narrow size distributions and average diameters up to ca. 10 μm were prepared under optimized polymerization conditions. The morphologies of the microspheres were characterized by nitrogen sorption porosimetry and the molecular recognition properties of representative products evaluated in high-performance liquid chromatography (HPLC) mode. Imprinting effects were confirmed by analyzing the relative retentions of the analytes on imprinted and non-imprinted packed HPLC columns. Finally, two different agitation/mixing methods for precipitation polymerizations were compared. It was found that the use of a low-profile roller housed inside a temperature-controlled incubator had advantages over a rotavapor-based system. Overall, this study has served to highlight the attractiveness of precipitation polymerization for the routine production of molecularly imprinted polymers in a well-defined spherical particulate form via an efficient one-step synthetic process.

Keywords: molecular imprinting; precipitation polymerization; HPLC; particle synthesis; xanthines.

INTRODUCTION

Molecular imprinting is a versatile and facile method for preparing synthetic polymers with predetermined molecular recognition properties [1–4] and, as such, is presently attracting widespread interest, especially as the technological value of molecularly imprinted polymers (MIPs) in chromatographic separations [5–7], biomimetic sensors [8–10], solid-phase extractions (SPEs) [11–13], and catalysis [14–16] has now been established clearly. One of the simplest methods available for MIP production in the laboratory involves conventional free-radical polymerization, wherein a monolith of a highly cross-

*Paper based on a presentation at the 12th International Conference on Polymers and Organic Chemistry 2006 (POC'06), 2–7 July 2006, Okazaki, Japan. Other presentations are published in this issue, pp. 1471–1582.

‡Corresponding author: E-mail: Peter.Cormack@strath.ac.uk

linked polymer forms upon copolymerization of functional monomer(s) with an excess of cross-linking agent in a porogenic solvent. Despite the relative simplicity of the practical chemistry therein, many variables have to be taken into account in the syntheses [17] and, indeed, high-throughput synthesis methods are being used increasingly to optimize the performance of the imprinted products in a time-efficient manner [18].

When discrete, imprinted polymer particles of a particular size range are desired, which is often the case, particularly for high-performance liquid chromatography (HPLC) and SPE work, grinding and sieving of the resultant monolith is necessary. Unfortunately, irregularly sized and shaped MIP particles are invariably obtained from grinding processes in low to moderate yields (typically <50 %), and there are drawbacks associated with the handling and application of such heterogeneous products. In order to streamline and optimize the production and performance of MIP particles, alternative synthetic strategies to discrete, imprinted, particulate products that obviate the need for grinding and sieving have evolved, including suspension polymerization [19,20], dispersion polymerization [21], and seeded polymerization [22,23]. Whilst these methods have undoubted value, optimization of reliable experimental protocols can be lengthy, the general applicability is questionable in some cases, and residual emulsifier or stabilizer can remain adsorbed on the particles' surfaces, potentially compromising selective rebinding of molecules to the imprinted material.

As an alternative to the above approaches, precipitation polymerization has emerged as an attractive, simple, and seemingly general method for producing high-quality, imprinted products as spherical particulates. Precipitation polymerization is a surfactant-free polymerization method that involves polymerization of monomers in dilute solution (typically <5 % w/v) in near-θ solvents [24–27]. Particle growth occurs predominantly via entropic precipitation of gel (seed) particles followed by continuous capture of oligomers from solution. Near monodisperse, spherical particles can be routinely prepared in good yields via this method. Furthermore, it is possible to tune the size and porosity of the particles through control of the polymerization conditions. Where precipitation polymerization has been applied to molecular imprinting, high-quality, imprinted spherical particulates have been obtained with diameters typically around 1 μm, especially for methacrylate-based materials, which have then been used in analytical techniques such as competition assays [27] and capillary electrochromatography (CEC) [28,29]. Until recently, it has proved difficult to produce larger imprinted monodisperse microspheres by precipitation polymerization with diameters that are better suited for direct application in high-performance chromatographic work or in SPE [30,31], however, in a recent communication we disclosed for the first time our ability to prepare monodisperse, molecularly imprinted, divinylbenzene (DVB)-based polymer microspheres with diameters of ca. 5 μm that were optimized for chemical analysis/separation applications [32]. The main objective of the present work, therefore, was to extend the scope for application of imprinted polymers prepared by precipitation polymerization through the evolution of reliable protocols for synthesizing spherical particulates with diameters in the micrometer size range. In this paper, the effects of solvent, functional monomer, cross-linker, and initiator concentrations were investigated, and molecularly imprinted spherical polymer particulates with narrow size distributions and average diameters prepared using either a rotavapor or a low-profile roller as the means of agitation/mixing. Whilst it is tricky to predict, a priori, the precise diameters of the spherical products produced by precipitation polymerization, the beaded products produced are normally in the size range 0.1–10 μm. Furthermore, size data obtained empirically for related polymerizations can be used to predict/control the size of the beaded products produced in subsequent preparations, often in a rational fashion. In the present work, the morphologies of the microspheres were determined by nitrogen sorption porosimetry and the molecular recognition properties of the imprinted materials confirmed by comparing the relative retentions of analytes on HPLC columns packed with imprinted and non-imprinted polymer microspheres.

EXPERIMENTAL SECTION

Materials

Methacrylic acid (MAA), 2-(trifluoromethyl)acrylic acid (TFMAA), α,α'-azobisisobutyronitrile (AIBN), divinylbenzene-80 (DVB, containing 80 % DVB isomers and 20 % ethyl vinylbenzene), caffeine, and theophylline were purchased from Aldrich UK. The inhibitor in DVB was removed by passing DVB through a column of activated aluminum oxide. MAA was purified by drying over anhydrous magnesium sulfate followed by distillation in vacuo. AIBN was purified by recrystallization from methanol. All solvents were of HPLC or analytical grade.

Preparation of polymers by precipitation polymerization

The polymers were prepared using methods adapted from those described by Li et al. [24–26], Ye et al. [27], and Wang et al. [32]. Theophylline and caffeine were used as model templates in the production of the imprinted materials. The experimental set-up used for the polymerizations is shown in Fig. 1, with the polymerizations being carried out either in a round-bottomed flask connected to a rotavapor (rotavapor method) or in a sealed high-density polyethylene (HDPE) bottle, or glass tube, rolled about its long axis on a low-profile roller (Stovall Life Science Inc., USA) in an incubator (Stuart Scientific, UK) (low-profile roller method). In a typical polymerization, fixed quantities of the template, MAA or TFMAA, DVB and AIBN, as shown in Table 1, were dissolved in the porogenic solvent in a round-bottomed flask or tube/bottle. The solution was degassed in an ultrasonic bath, sparged with oxygen-free nitrogen for 10 min while cooling on an ice bath, and attached either to the rotavapor or sealed with a screw cap in the case of a tube or bottle. The temperature of the oil bath (rotavapor method) or the incubator (low-profile roller method) was increased from room temperature to 60 °C over a period of 2 h, and then held at 60 °C for a further 24 h. At the end of this period, the polymer particles were separated from the reaction medium simply by filtration on a 0.2 μm nylon membrane filter, washed sequentially with methanol containing 20 % (v/v) acetic acid (100 mL) and methanol (100 mL), and then dried in vacuo overnight at 40 °C. The isolated yields of all the particles prepared in this way were determined gravimetrically.

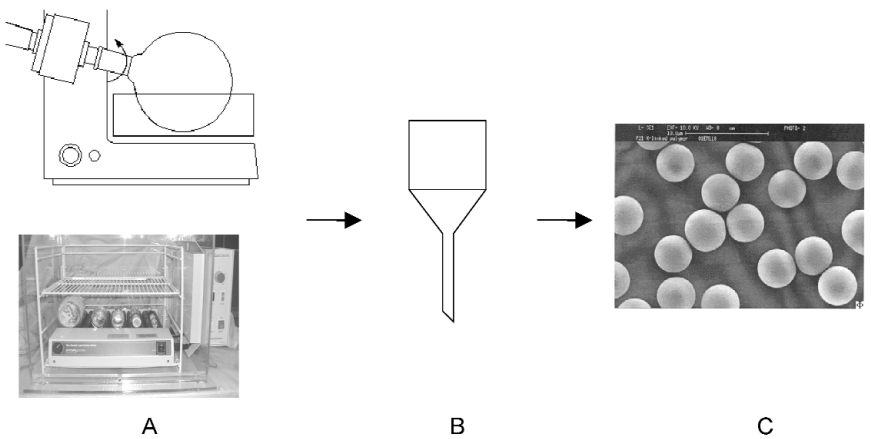

Fig. 1 Typical precipitation polymerization procedures. (A) Polymerizations are carried out either in a round-bottomed flask connected to a rotavapor (upper image) or in a sealed glass tube or bottle rolled around its long axis on a low-profile roller in an incubator (lower image). (B) At the end of the reaction, the microspheres are separated from the reaction medium simply by filtration on a 0.2 μm nylon membrane filter, washed successively with methanol containing 20 % (v/v) acetic acid (100 mL) and methanol (100 mL), and then dried in vacuo overnight at 40 °C. (C) The microspheres are ready for immediate use, e.g., in SPE or HPLC applications.

Table 1 Precipitation polymerization feed compositions.

Polymer	Template (mmol)	Functional monomer (mmol)	DVB (mmol)	Solvent	(mL)	AIBN (%)[b]
P1	–[a]	TFMAA (0.50)	2.40	Chloroform (22)	–	1
P2	–[a]	TFMAA (0.50)	2.40	Chloroform (15.4)	Hexane (6.6)	1
P3	–[a]	TFMAA (0.50)	2.46	Chloroform (6.6)	Hexane (15.6)	1
P4	–[a]	TFMAA (0.50)	2.40	Acetonitrile (22)	–	1
P5	Caffeine (0.36)	TFMAA (1.57)	7.07	Acetonitrile (50)	Toluene (17)	1
P6	–[a]	–	3.44	Acetonitrile (22.5)	Toluene (7.5)	1
P7	–[a]	MAA (1.63)	7.20	Acetonitrile (48)	Toluene (16)	1
P8	Caffeine (0.36)	MAA (1.63)	7.20	Acetonitrile (48)	Toluene (16)	1
P9	Caffeine (0.77)	MAA (3.0)	14.4	Acetonitrile (44)	Toluene (15)	1
P10	–[a]	MAA (3.0)	14.4	Acetonitrile (96)	Toluene (32)	3
P11	–[a]	MAA (6.0)	28.8	Acetonitrile (96)	Toluene (32)	3
P12	Caffeine (1.5)	MAA (6.0)	28.8	Acetonitrile (96)	Toluene (32)	3
P13	Theophylline (1.5)	MAA (6.0)	28.8	Acetonitrile (96)	Toluene (32)	3
P14	Caffeine (0.6)	MAA (2.3)	11.1	Acetonitrile (36.9)	Toluene (12.3)	3
P15[c]	Caffeine (0.95)	MAA (3.7)	17.7	Acetonitrile (59.1)	Toluene (19.7)	3
P16	Theophylline (0.6)	MAA (2.3)	11.1	Acetonitrile (36.9)	Toluene (12.3)	3
P17	Theophylline (0.6)	MAA (2.3)	11.1	Acetonitrile (36.9)	Toluene (12.3)	3
P18	Theophylline (0.35)	MAA (1.4)	6.6	Acetonitrile (22.2)	Toluene (7.4)	3

[a]No template present, i.e., non-imprinted control polymer.
[b]With respect to the total number of moles of polymerizable double bonds.
[c]P15-I-1, P15-I-2, and P15-I-3 were also prepared using the low-profile roller method. The reaction volumes for P15-I-1, P15-I-2, and P15-I-3 were 10 mL in each case, and were aliquoted directly from the P15 stock solution prior to polymerization.

Particle size and shape

The particle size distributions of the polymer microspheres were measured using a Coulter Counter (Model TA, Coulter Electronics Ltd, UK) with Isoton II as the electrolyte. Selected microspheres were also imaged using the scanning electron microscope (SEM) facility at Unilever Research (Port Sunlight, UK) or at the University of Glasgow (Glasgow, UK).

Polymer morphology

Porosity and surface area analyses were performed by nitrogen sorption porosimetry on a Micromeritics ASAP 2000 instrument. Generally speaking, a polymer sample of around 0.3–0.4 g was degassed at 100 °C overnight in vacuo and the morphology then established on the basis of the nitrogen uptake and application of the Brunauer–Emmett–Teller (BET) theory.

HPLC evaluation of the polymers

Using an air-driven fluid pump, polymer microspheres P11, P12, and P13 were slurried and packed with acetone as the slurry and distribution solvent into 2.1 I.D. × 125 mm stainless steel HPLC columns at 3000 psi. The chromatograms were obtained using a Waters 717 autosampler, Waters 600 controller, and Waters 2487 dual λ UV detector and data collected and manipulated using Waters Millennium[32] software. Acetone was used as the void marker. 2.5 μg of analyte in 10 μL chloroform were injected onto the columns and retention factors (k') calculated according to standard chromatographic theory (eq. 1):

$$k_1' = (t_1 - t_0)/t_0 \quad (1)$$

where t_0 and t_1 are the retention times of the void marker and the analyte, respectively.

RESULTS AND DISCUSSION

Effect of functional monomer and solvent on the formation of the microspheres

During the course of recent work involving the production of imprinted materials in monolithic form, which will be published elsewhere in full in due course, we discovered that copolymers based upon DVB and TFMAA could be imprinted very effectively using caffeine as a model template. Furthermore, we found that chloroform was a better porogenic solvent than acetonitrile for such copolymerizations, as judged from the molecular recognition properties of the resultant copolymers. In contrast, the group of Stöver [25] has reported that acetonitrile, or mixtures of acetonitrile with toluene, are effective porogens (near-θ solvents) for precipitation polymerizations involving DVB and give rise to high-quality beaded products in reasonable yields. Undeterred, we initially attempted to use chloroform as a solvent for precipitation polymerizations involving DVB and TFMAA as comonomers, either by itself or as a cosolvent with hexane. However, phase separation was not apparent to the naked eye after polymerization for 24 h under such conditions (Table 1, P1). When hexane was introduced as a cosolvent (P2 and P3), macrogelation was observed 25 min after the reaction temperature reached 60 °C, which was indicative of early phase separation and in line with what one would expect when using thermodynamically poorer porogenic solvents. Interestingly, upon moving to acetonitrile or acetonitrile/toluene as the solvent (P4 and P5), once again phase separation did not occur over the course of the polymerizations. We ascribed these results to the presence of TFMAA, and in particular to the effects it was having upon the solubility parameter of the oligomers generated continuously throughout the course of the precipitation polymerizations [33]. Similar phenomena (macrogelation and soluble polymer formation) were reported by Goh et al. for poly(MAA-*co*-poly(ethylene oxide) methyl ether methacrylate) polymers prepared by precipitation polymerization; Goh et al. established a "morphology map" to predict the morphology of the polymers formed as a function of the monomers and solvents used, as well as the experimental conditions [34]. By following a similar line of reasoning, we expected that by moving to a less polar acidic comonomer, and thus closer to the θ-state, we could generate the desired beaded products. This turned out to be the case.

MAA has been used extensively for noncovalent molecular imprinting protocols and, significantly, has been shown to be useful for caffeine imprinting [35–37]. MAA was therefore chosen as an alternative monomer to TFMAA in our subsequent experiments. PolyDVB-55 microspheres prepared via precipitation polymerization in neat acetonitrile show negligible porosity and very low specific surface areas [25]. Introduction of toluene as a cosolvent improves the compatibility of the oligomers with the solvent, resulting in later phase separation during the polymerization and significant increases in the specific surface areas and the total pore volumes of the beaded products [25]. In order to prepare MIPs with reasonable surface areas and porosities, a mixture of 75 % acetonitrile and 25 % toluene (v/v) as the porogenic solvent was therefore employed in combination with DVB-80 as the cross-linking agent. Maintaining the concentration of monomer(s) at 2 % (w/v) relative to the total volume of solvent and the concentration of initiator, AIBN, at 1 mol % with respect to the total number of moles of polymerizable double bonds, polymerizations were carried out either in the absence of MAA (P6) or in the presence of MAA (P7 and P8) as the comonomer. Pleasingly, all three polymerizations gave rise to beaded products, albeit in modest yields. Comparing P6 with P7 reveals that introduction of MAA as the comonomer increases the yield of isolated product but lowers the average particle diameter (Table 2, Fig. 2). The monomer feed compositions for P7 and P8 were identical except that no caffeine was present for P7, i.e., P7 is a non-imprinted control polymer. However, the presence of caffeine during the P8 polymerization dramatically reduced the average particle size of the products, possibly due to modulation of the reactivity ratios of the monomers and/or the solvency power, impacting upon the precipita-

tion polymerization, such that they were too small to be measured by a Coulter Counter with an orifice tube of 100 μm aperture. They were thus too small also for the analytical applications proposed (LC and SPE), therefore, a means had to be found to increase the particle size of products formed in the presence of caffeine.

Table 2 Effect of the concentration of monomers and initiator on the diameter and yield of the polymer products.

Polymer	Concentration of monomer (%)[a]	Concentration of initiator (%)[b]	Average diameter (μm)	Yield (%)
P6	2	1	5.42	27
P7	2	1	3.95	47
P8	2	1	–[c]	29
P9	4	1	3.53	9
P10	2	3	–[d]	22
P11	4	3	5.36	62
P12	4	3	9.50	62
P13	4	3	4.27	55

[a]With respect to porogenic solvent (w/v).
[b]With respect to the number of moles of polymerizable double bonds.
[c]The average diameter of P8 was too small to be measured by a Coulter counter using an orifice tube with an aperture of 100 μm, and is believed to be less than 1.0 μm.
[d]The size distribution of P10 was too wide to be measured by a Coulter counter using an orifice tube with an aperture of 100 μm.

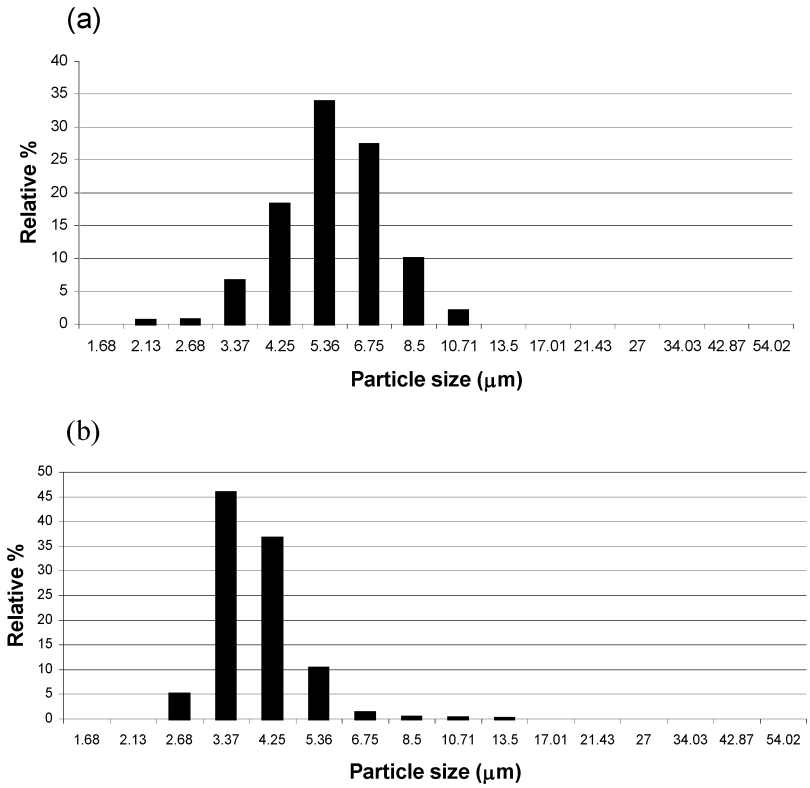

Fig. 2 Particle size distribution of: (a) P6 and (b) P7.

Effect of monomer and initiator concentration on particle size and yield

To investigate the effect of independently changing the concentration of monomers and initiator on the outcome of the polymerizations, P9 and P10 were synthesized. Keeping the concentration of AIBN constant at 1 mol %, whilst increasing the concentration of monomers from 2 to 4 % (w/v), resulted in an increase in the average particle diameter (c.f. P8 and P9, Fig. 3 and Table 2) whereas the yield of microspheres dropped from 29 to 9 %. In contrast, when the concentration of monomers was kept constant at 2 %, increasing the AIBN concentration from 1 mol % (P7) to 3 mol % (P10) gave rise to a higher flux of radicals, a lower yield, and a very wide particle size distribution. However, when the concentrations of the monomers and initiator were increased simultaneously, polymer microspheres (P11, P12, and P13) with significantly larger average diameters and narrow size distributions were obtained in good yields, both in the presence and the absence of the template (Table 2, Fig. 4). This seems to be the key in preparing beaded polymers in good yields and diameters appropriate for affinity separation applications. The narrow size distributions of P11, P12, and P13 were confirmed by SEM analyses (Fig. 5).

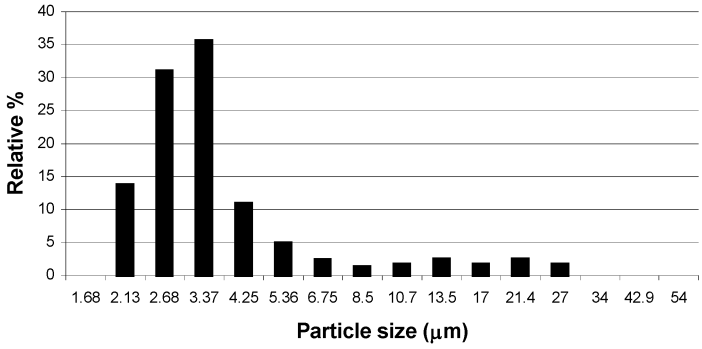

Fig. 3 Particle size distribution of P9.

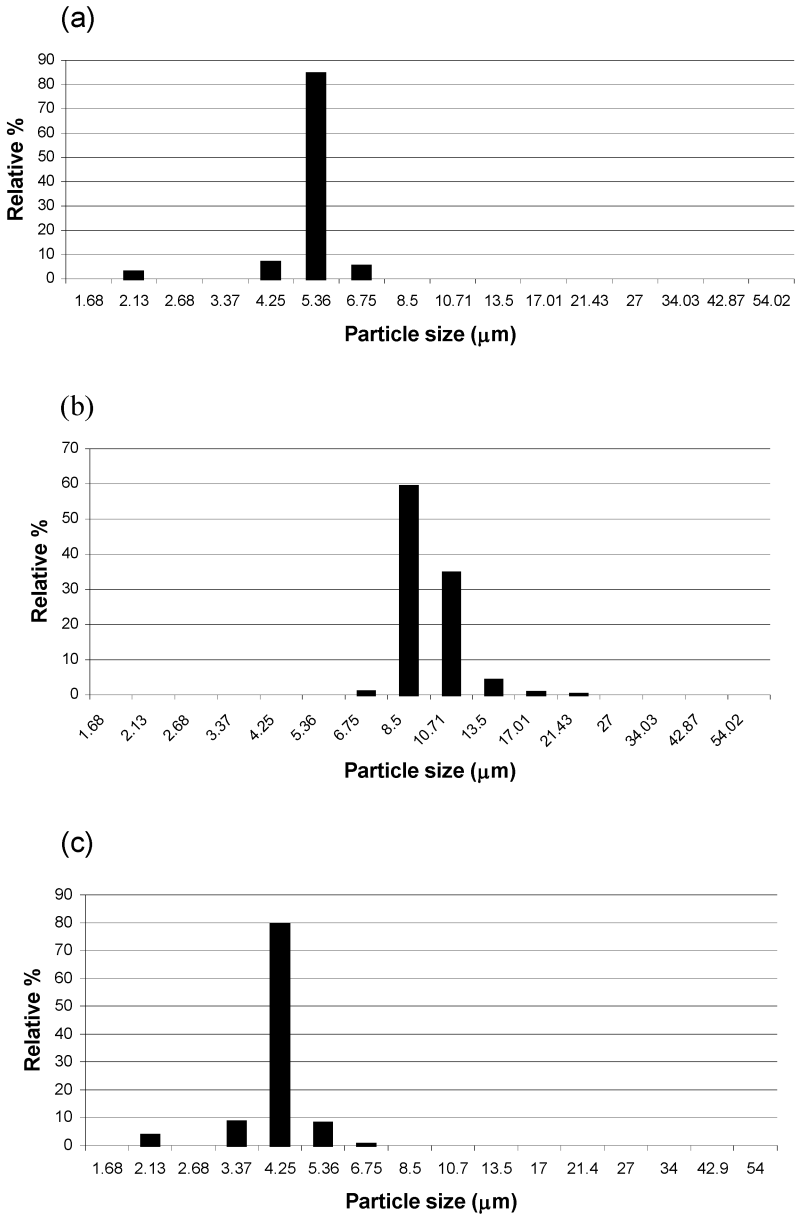

Fig. 4 Particle size distributions of: (a) P11, (b) P12, and (c) P13.

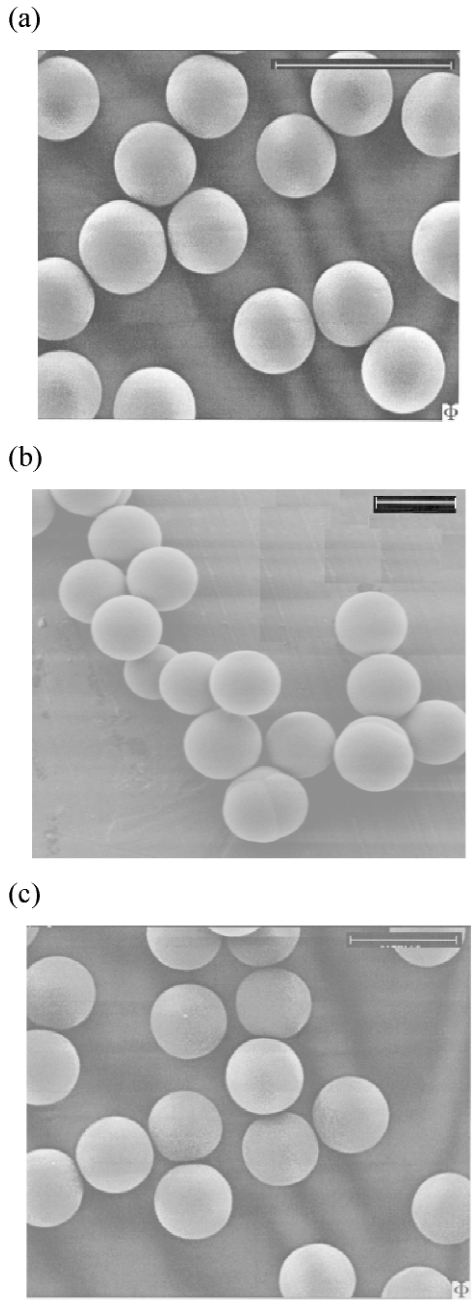

Fig. 5 SEMs of: (a) non-imprinted microspheres (P11) (bar = 10 μm); (b) caffeine-imprinted microspheres (P12) (bar = 10 μm); and (c) theophylline-imprinted microspheres (P13) (bar = 5 μm).

Molecular recognition properties of the molecularly imprinted microspheres

The retention behavior of caffeine and theophylline on HPLC columns packed with P11, P12, and P13, respectively, were investigated. When chloroform was used as the mobile phase, the retention factor of caffeine on P11 and P12 was 0.78 and 1.15, respectively, which, when taken together with the asymmetrical elution profile of caffeine on P12, is indicative of the fact that P12 is imprinted with caffeine

(Table 3). The retention factor of theophylline on P11 was 2.37, whereas theophylline was completely retained by P12 when chloroform was employed as the mobile phase. This result shows that P12, which was imprinted with caffeine, shows strong cross-selectivity for the caffeine analog theophylline. The same trend was observed when acetonitrile was employed as the mobile phase.

Table 3 Retention factors of caffeine and theophylline on P11, P12, and P13.

	P11	P12	P13
k'_{caffeine}	0.80[a]	0.91[a]	0.87[a]
	0.78[b]	1.15[b]	1.02[b]
$k'_{\text{theophylline}}$	2.43[a]	2.64[a]	5.39[a]
	2.37[b]	CR[b]	CR[b]

[a]Mobile phase: acetonitrile, flow rate: 0.5 mL/min; detection: 270 nm. 2.5 μg in 10 μL chloroform was injected.
[b]Mobile phase: chloroform; flow rate: 0.5 mL/min; detection: 270 nm. 2.5 μg in 10 μL chloroform was injected.
CR = completely retained.

With acetonitrile as the mobile phase, the retention factor of theophylline on P11 and P13 was 2.42 and 5.39, respectively, and, furthermore, there was extensive peak tailing of theophylline on P13 (Fig. 6). This supports the assertion that P13 is imprinted. From Table 3, it can also be seen that P13 (a theophylline imprint) shows cross-selectivity for caffeine when both chloroform and acetonitrile are applied as the mobile phase.

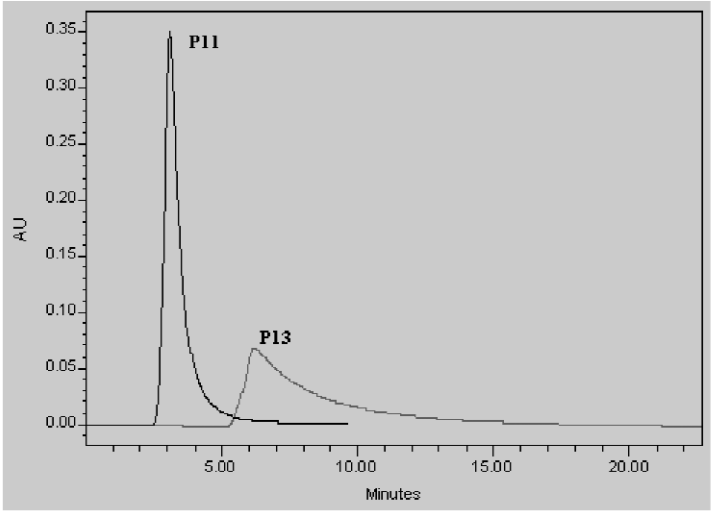

Fig. 6 Comparison of theophylline retention on P11 and P13. Mobile phase: acetonitrile, flow rate: 0.5 mL/min, detection: 270 nm. 2.5 μg theophylline in 10 μL chloroform was injected.

The retention factor of theophylline on non-imprinted P11 is relatively larger than that of caffeine, which suggests that the nonspecific interactions between theophylline and P11 are stronger than those between caffeine and P11. These nonspecific interactions are believed to give rise to the stronger re-

tention of theophylline on P12, compared to caffeine, even although caffeine was the template used in the production of P12. We have observed a similar phenomenon for caffeine- and theophylline-imprinted polymers prepared by conventional polymerization methods in the form of monoliths (unpublished data).

Method of mixing/agitation

Polymers P1–P13 were prepared via the rotavapor method, and we were keen to assess the utility of the low-profile roller method for the routine production of polymer microspheres. Accordingly, three replicate polymerizations were carried out using the rotavapor method (P12, P14, and P15) and three replicate polymerizations were carried out using the low-profile roller method (P15-I-1, P15-I-2, and P15-I-3). The monomer feed ratios and concentrations used were identical in all six polymerizations (Table 1). Pleasingly, all six polymerizations gave rise to good yields of polymer products in the form of spherical particulates with narrow size distributions (Table 4).

Table 4 Caffeine- and theophylline-imprinted polymer microspheres prepared using the rotavapor and low-profile roller methods.

Polymer	Template	Average diameter (μm)	Yield (%)	Apparatus
P11	–	5.36	62	Rotavapor
P12	Caffeine	9.50	62	Rotavapor
P13	Theophylline	4.27	55	Rotavapor
P14	Caffeine	3.22	44	Rotavapor
P15	Caffeine	3.99	43	Rotavapor
P15-I-1	Caffeine	2.99	55	Roller
P15-I-2	Caffeine	3.00	55	Roller
P15-I-3	Caffeine	2.95	55	Roller
P16	Theophylline	3.06	65	Roller
P17	Theophylline	2.97	67	Roller
P18	Theophylline	3.06	63	Roller

Figure 7 shows SEM images of P15 and P15-I-2, respectively. The particle size distributions of P15-I-1, P15-I-2, and P15-I-3 are shown in Fig. 8. Upon comparing the average particle diameters of P12, P14, P15, P15-I-1, P15-I-2, and P15-I-3 (Table 4), it is clear that the polymer microspheres obtained using the low-profile roller method are marginally smaller than those obtained using the rotavapor method, however, the particle size distributions of P15-I-1, P15-I-2, and P15-I-3 are narrower and have high reproducibility (Table 4 and Fig. 8). The yields of P15-I-1, P15-I-2, and P15-I-3 were all identical (55 %) and a little higher than for P14 and P15, albeit a little lower than for P12. Theophylline-imprinted P16, P17, and P18, prepared using the low-profile roller method, were spherical particulates with slightly lower average particle diameters and higher yields compared to P13 (Fig. 9 and Table 4). These results highlight our belief that the low-profile roller method is superior to the rotavapor method for the preparation of imprinted polymer microspheres in terms of yields, reproducibility of the particle diameters, and particle size distributions.

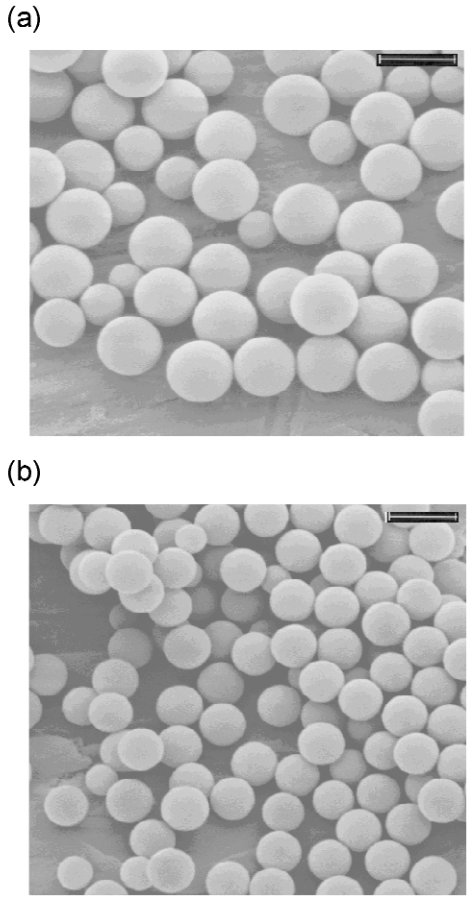

Fig. 7 SEMs of: (a) caffeine-imprinted polymer microspheres (P15) prepared using the rotavapor method (bar = 5 μm), and (b) caffeine-imprinted polymer microspheres (P15-I-2) prepared using the low-profile roller method (bar = 5 μm).

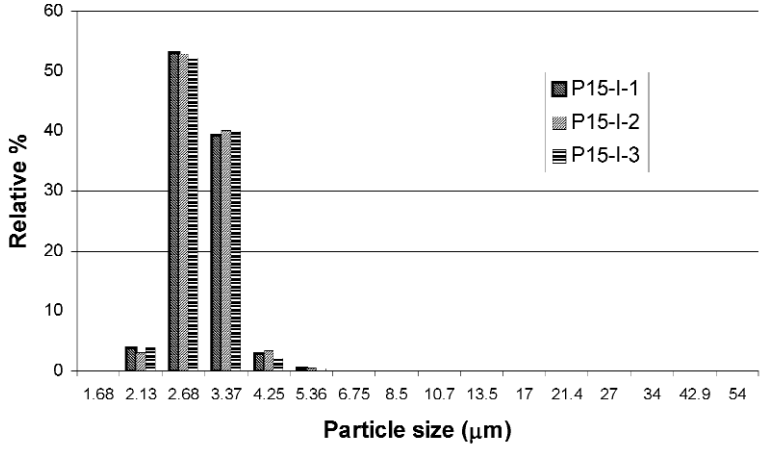

Fig. 8 Particle size distributions of P15-I-1, P15-I-2, and P15-I-3.

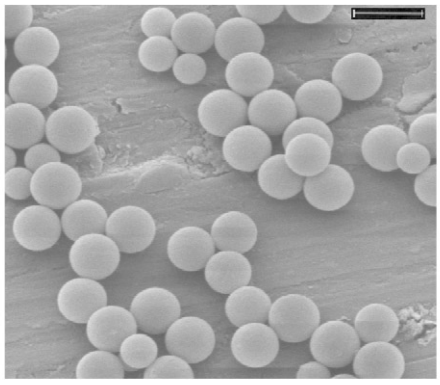

Fig. 9 SEM of theophylline-imprinted polymer microspheres (P16) prepared using the low-profile roller method (bar = 5 μm).

Morphology of the polymers

P11 was prepared in the absence of template, whereas P12 and P13 were prepared with caffeine and theophylline as the templates, respectively. Since P11, P12, and P13 were prepared using high levels of cross-linker and in the presence of a thermodynamically good solvent (toluene), it was expected that they would be macroporous, and indeed this turned out to be the case. All three polymers had similar properties in terms of their average pore diameters, specific pore volumes, specific micropore volumes, and specific micropore areas, which suggested that the presence of template during the polymerizations did not dramatically affect the morphologies of the resultant polymers (Table 5). P11, P12, and P13 all show high specific surface areas and a large portion of micropores, in contrast to polyDVB-55 microspheres prepared in neat acetonitrile, which have been reported to show negligible porosity and very low specific surface areas [25]. According to the proposed mechanism of precipitation polymerization, seed particles are well swollen by the solvent and capture soluble oligomers continuously from solution [26]. The solubility parameters for acetonitrile, toluene, and polyDVB are 24.6, 18.6, and ~17–18 $MPa^{0.5}$, respectively [38–39]. When neat acetonitrile is used as the solvent, there is a mis-match between the solubility parameter of the solvent and the polymer, leading to early phase separation of polymer from the monomer phase, poor solvation of the polymer phase by the solvent, and therefore products with negligible porosity and very low specific surface areas [25]. However, when DVB is copolymerized with MAA in a mixture of acetonitrile and toluene, there is a much better match between the solubility parameter of the solvent and the polymer, leading to better solvation of the polymer and well-developed pore structure and high specific surface areas (Table 5). In effect, toluene serves to promote pore formation.

Since polymers P11–P16 had similar feed compositions and were produced via the same precipitation polymerization mechanism, it is not surprising that the morphologies of polymers prepared by the rotavapor method and the low-profile roller method are rather similar, e.g., compare P13 and P16 for theophylline imprinting and P12, P15, P15-I-2, and P15-I-3 for caffeine imprinting.

Table 5 Morphology of the polymer microspheres.

Polymer	BET specific surface area[a] (m^2/g)	Specific pore volume[b] (cm^3/g)	Average pore diameter[c] (nm)	Specific micropore volume[d] (cm^3/g)	Specific micropore area[d] (m^2/g)
P11	656	0.155	2.85	0.111	285
P12	702	0.187	2.85	0.105	240
P13	554	0.131	2.92	0.100	224
P15	672	0.169	2.91	0.110	248
P15-I-2	633	0.160	3.00	0.118	267
P15-I-3	660	0.169	2.99	0.121	273
P16	735	0.163	2.97	0.144	321

[a]Determined using the BET model on an eight-point linear plot.
[b]BJH cumulative adsorption pore volume of pores between 1.7 and 300 nm.
[c]BJH adsorption average pore diameter (4 × pore volume/surface area) of pores between 1.7 and 300 nm.
[d]Based on a t-plot using Harkins–Jura average thickness.

CONCLUSIONS

MIPs in the form of spherical particulates have been prepared by precipitation polymerization and the effects of changing the solvent, monomer, and initiator concentrations on the outcome of the polymerizations investigated. The yields of the MIPs could not be increased by increasing the concentrations of initiator or monomer independently, whereas the yields could be increased by simultaneously increasing the concentrations of initiator and monomer. Typical monomer feeds were 3 % (w/v), relative to the solvent, and typical initiator concentrations were 2 mol %. Polymer microspheres with narrow size distribution and average diameters up to 9.5 μm could be prepared under optimized polymerization conditions. The morphologies of the resultant microspheres were characterized by nitrogen sorption porosimetry, and the molecular imprinting properties of selected microspheres evaluated in HPLC mode. Caffeine and theophylline imprinting effects were confirmed by analyzing the retention behavior of theophylline and caffeine on imprinted and non-imprinted HPLC columns. The low-profile roller method showed advantages over the rotavapor method in that the reproducibility of the particle size distribution was better and the yields of the microspheres were higher. Furthermore, because up to around 20 reaction vessels, each with a volume of 50 mL, can be placed on a single low-profile roller and polymerized simultaneously, this represents a very convenient route to optimize the polymerization conditions in molecular imprinting by parallel and/or combinatorial chemistry methods. Clearly, the reaction volume can be reduced substantially (e.g., from 50 to 1 mL), if so desired, to enable the yet higher throughput of chemically distinct materials. Overall, this study has served to highlight the attractiveness of precipitation polymerization for the routine preparation of MIPs in a well-defined spherical particulate form via an efficient one-step synthetic process.

ACKNOWLEDGMENT

This work was supported in part by Unilever Research.

REFERENCES

1. K. Mosbach, O. Ramström. *Bio/Technology* **14**, 163 (1996).
2. G. Wulff. *Angew. Chem., Int. Ed. Engl.* **34**, 1812 (1995).
3. K. J. Shea. *Trends Polym. Sci.* **2**, 166 (1994).
4. O. Brüggemann, K. Haupt, L. Ye, E. Yilmaz, K. Mosbach. *J. Chromatogr., A* **889**, 15 (2000).

5. M. Kempe, K. Mosbach. *J. Chromatogr., A* **649**, 3 (1995).
6. B. Sellergren. *J. Chromatogr., A* **906**, 227 (2001).
7. K. Haupt. *Analyst* **126**, 747 (2001)
8. D. Kriz, O. Ramström, K. Mosbach. *Anal. Chem*. **69**, A345 (1997).
9. S. A. Piletsky, Y. P. Parhometz, N. V. Lavryk, T. L. Panasyuk, A. V. Elskaya. *Sens. Actuators, B* **19**, 629 (1994).
10. K. Haupt, K. Mosbach. *Chem. Rev.* **100**, 2495 (2000).
11. F. Lanza, B. Sellergren. *Chromatographia* **53**, 599 (2001).
12. D. Stevenson. *Trends Anal. Chem.* **18**, 154 (1999).
13. L. I. Andersson. *J. Chromatogr., B* **739**, 163 (2000)
14. G. Wulff. *Chem. Rev.* **102**, 1 (2002).
15. M. J. Whitcombe, C. Alexander, E. N. Vulfson. *Synlett* **6**, 911 (2000).
16. C. Alexander, L. Davidson, W. Hayes. *Tetrahedron* **59**, 2025 (2003).
17. O. Ramström. In *Molecularly Imprinted Materials: Science and Technology*, M. Yan, O. Ramström (Eds.), pp. 181–224, Marcel Dekker, New York (2005).
18. F. Lanza, B. Sellergren. *Anal. Chem*. **71**, 2092 (1999).
19. A. G. Mayes, K. Mosbach. *Anal. Chem*. **68**, 3769 (1996).
20. A. Flores, D. Cunliffe, M. J. Whitcombe, E. N. Vulfson. *J. Appl. Polym. Sci.* **77**, 1841 (2000).
21. B. Sellergren. *Anal. Chem.* **66**, 1578 (1994).
22. K. Hosoya, Y. Shirasu, K. Kimata, N. Tanaka. *Anal. Chem.* **70**, 943 (1998).
23. E. Yilmaz, O. Ramström, P. Moller, D. Sanchez, K. Mosbach. *J. Mater. Chem.* **12**, 1577 (2002).
24. K. Li, H. D. H. Stöver. *J. Polym. Sci., Part A: Polym. Chem.* **31**, 3257 (1993).
25. W. H. Li, H. D. H. Stöver. *J. Appl. Polym. Sci., Part A: Polym. Chem.* **36**, 1543 (1998).
26. W. H. Li, K. Li, H. D. H. Stöver. *Macromolecules* **33**, 4354 (2000).
27. L. Ye, P. A. G. Cormack, K. Mosbach. *Anal. Commun*. **36**, 35 (1999).
28. T. de Boer, R. Mol, R. A. de Zeeuw, G. J. de Jong, D. C. Sherrington, P. A. G. Cormack, K. Ensing. *Electrophoresis* **23**, 1296 (2002).
29. L. Schweitz, P. Spégel, S. Nilsson. *Analyst* **125**, 1899 (2000).
30. P. Li, F. Rong, C. W. Yuan. *Polym. Int*. **52**, 1799 (2003).
31. Y. Jiang, A. J. Tong. *J. Appl. Polym. Sci*. **94**, 542 (2004).
32. (a) J. F. Wang, P. A. G. Cormack, D. C. Sherrington, E. Khoshdel. *Angew. Chem., Int. Ed. Engl.* **42**, 5336 (2003); (b) J. F. Wang, P. A. G. Cormack, D. C. Sherrington, E. Khoshdel. *Angew. Chem.* **115**, 5494 (2003).
33. J. S. Downey, R. S. Frank, W. H. Li, H. D. H. Stöver. *Macromolecules* **32**, 2838 (1999).
34. C. C. Goh, H. D. H. Stöver. *Macromolecules* **35**, 9983 (2002).
35. C. Baggiani, F. Trotta, G. Giraudi, G. Moraglio, A. Vanni. *J. Chromatogr., A* **786**, 23 (1997).
36. C. Liang, H. Peng, X. Bao, L. Nie, S. Yao. *Analyst* **124**, 1781 (1999).
37. F. A. Villamena, A. A. de la Cruz. *J. Appl. Polym. Sci*. **82**, 195 (2001).
38. D. C. Sherrington. *Chem. Commun*. 2275 (1998).
39. J. Brandrup, E. H. Immergut. *Polymer Handbook*, 3rd ed., pp. VII, 519, Wiley-Interscience, New York (1989).